

77039

77039

P12

NASA Technical Memorandum 4365

# Singularities in Optimal Structural Design

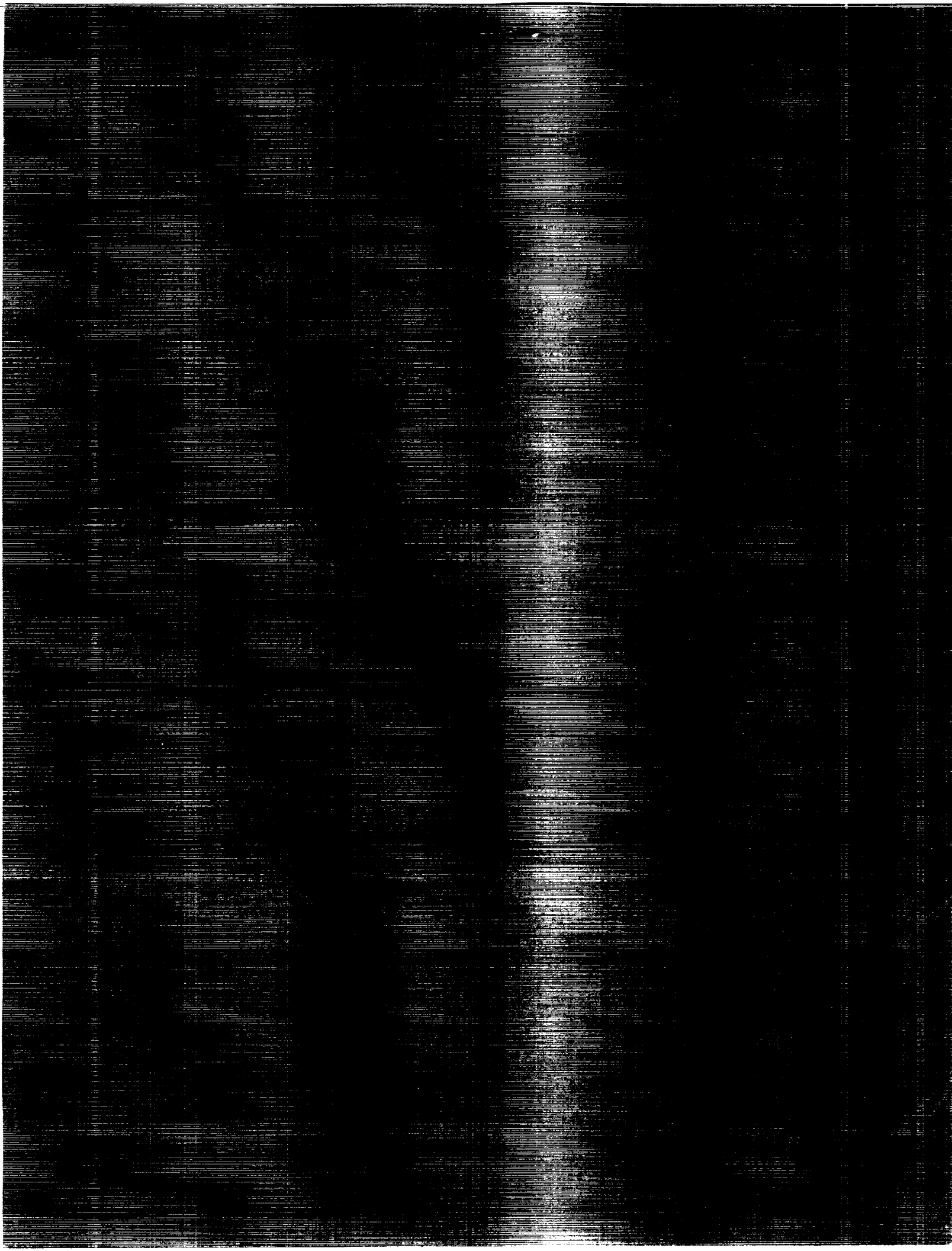
N. Patnaik  
and L. Berke

MARCH 1992

(NASA-TM-4365) SINGULARITIES IN OPTIMAL STRUCTURAL DESIGN (NASA) 12 p CSCL 20K

77039

Unclas  
H1/39 0077039



NASA Technical Memorandum 4365

# Singularities in Optimal Structural Design

S. N. Patnaik  
*Ohio Aerospace Institute*  
*Brook Park, Ohio*

J. D. Guptill and L. Berke  
*Lewis Research Center*  
*Cleveland, Ohio*



National Aeronautics and  
Space Administration  
Office of Management  
Scientific and Technical  
Information Program

1992



## Summary

Singularity conditions that arise during structural optimization can seriously degrade the performance of the optimizer. The singularities are intrinsic to the formulation of the structural optimization problem and are not associated with the method of analysis. Certain conditions that give rise to singularities have been identified in earlier papers, along with a proposition to alleviate the consequences of their presence (refs. 1 to 3). These singularities were global in nature, encompassing the entire structure. Further examination revealed more complex sets of conditions in which singularities occur. Some of these singularities are local in nature, being associated with only a segment of the structure. Moreover, the likelihood that one of these local singularities may arise during an optimization procedure can be much greater than that of the global singularity identified earlier. This paper provides examples of these additional forms of singularities. It also gives a framework in which these singularities can be recognized. In particular, the singularities can be identified by examination of the stress-displacement relations along with the compatibility conditions and/or the displacement-stress relations derived in the integrated force method of structural analysis.

## Introduction

Structural optimization methodologies based on mathematical programming techniques require constraint-gradient information (ref. 4). Nonlinear optimization proceeds iteratively, and at each iteration a direction vector  $\bar{\phi}$  is generated in the design variable space. The formation of this direction vector utilizes the gradients. Consider, for example, the coefficient matrix  $[H]$  used in a method of feasible directions, as given by Best, (ref. 4) to find the direction vector

$$\phi = \frac{[H]\bar{\nabla}f}{2\lambda_0} \quad (1)$$

where

$$[H] = [I] - [\nabla g] \left[ [\nabla g]^T [\nabla g] \right]^{-1} [\nabla g]^T \quad (2)$$

$$[\nabla g] = \begin{bmatrix} \frac{\partial g_1}{\partial \chi_1} & \frac{\partial g_2}{\partial \chi_1} & \cdots & \frac{\partial g_\kappa}{\partial \chi_1} \\ \frac{\partial g_1}{\partial \chi_2} & \frac{\partial g_2}{\partial \chi_2} & \cdots & \frac{\partial g_\kappa}{\partial \chi_2} \\ \vdots & \vdots & \ddots & \vdots \\ \frac{\partial g_1}{\partial \chi_n} & \frac{\partial g_2}{\partial \chi_n} & \cdots & \frac{\partial g_\kappa}{\partial \chi_n} \end{bmatrix} \quad (3)$$

where  $\bar{\nabla}f$  is the gradient of the merit function,

$$\lambda_0 = -0.5 \sqrt{[H]\bar{\nabla}f]^T [H]\bar{\nabla}f} \quad (4)$$

and  $\kappa$  is the number of active constraints used in the computation of the direction vector.

In equation (3),  $\chi_i$  represents the  $i$ th design variable, and  $g_j$  represents the  $j$ th constraint value (e.g., the nondimensionalized element stress or nodal displacement). Here, we consider only sizing design variables (e.g., the cross-sectional areas of truss elements).

Now, if the rank of the gradient matrix  $[\nabla g]$  is less than  $\kappa$ , then the derived composite matrix  $[[\nabla g]^T [\nabla g]]$  will be singular. Thus, the coefficient matrix  $[H]$  is not defined, and any direction generated from equation (1) would be spurious. Gradient projection methods that use the matrix  $[H]$  can suffer the same consequences, and similar remarks can be made about other techniques that use constraint-gradient information in this way. Computer codes can react to this situation by premature termination (sometimes with indications of multiple overflow errors) or divergence. These observations are intrinsic to the specification of the constraint formulation in the structural optimization problem and are not associated with any specific analyzer.

Clearly, the rank of the gradient matrix  $[\nabla g]$  is less than or equal to the smaller of the number of active constraints  $\kappa$  and the number of design variables  $n$ . Thus, whenever the

number of active constraints is larger than the number of design variables, the rank of  $[\nabla g]$  will be less than  $\kappa$  (since  $n < \kappa$ ), and singularities in  $[H]$  will occur. However, as pointed out earlier (refs. 1 to 3), whenever the number of active stress and displacement constraints is more than the number of displacement degrees of freedom of the structure (which is often significantly less than  $n$ ), singularities will also be introduced. This condition depends only on the number of active constraints, irrespective of where on the structure the active constraints appear, and will be referred to as a global singularity condition.

## Linear Functional Dependence Among Constraints

Constraint sets formed during structural optimization may exhibit functional dependence. Moreover, this functional dependence may be linear in form. That is, for certain sets of constraint functions of the design variable  $\bar{\chi}$  (e.g.,  $\{g_1(\bar{\chi}), g_2(\bar{\chi}), \dots, g_\kappa(\bar{\chi})\}$ ), there exists a set of constants  $\{\alpha_j\}$ , not all zero, such that

$$\sum_{j=1}^{\kappa} \alpha_j g_j(\bar{\chi}) = 0 \quad \text{for all } \bar{\chi} \quad (5)$$

Note that any individual function  $g_j(\bar{\chi})$  may be nonlinear in the independent variable  $\bar{\chi}$ . This linear functional dependence, in turn, generates linear dependence among constraint gradients (which leads to singularities). Differentiating equation (5) with respect to  $\bar{\chi}$  gives

$$\sum_{j=1}^{\kappa} \alpha_j \nabla g_j = 0 \quad (6)$$

where  $\nabla g_j$  is the gradient of the function  $g_j$  with respect to  $\bar{\chi}$ .

## Constraint Dependence for a Three-Bar Truss

To illustrate the existence and importance of linear functional dependence among constraints, consider a three-bar steel truss with a Young's modulus  $E$  of 30 000 ksi and a strength  $\sigma_0$  of 20 ksi (fig. 1). For each load condition, the truss can have three stress and two displacement constraints. The stresses and displacements are functions of the cross-sectional areas of the bar elements  $\bar{\chi}$  and either (or both) type(s) of constraints may appear in the active constraint set. It can be shown that, for the three-bar truss, the following relationships hold for each load condition:

$$X_1 = \left(\frac{1}{E}\right) (\ell\sigma_2 - 2\ell\sigma_1) \quad (7a.1)$$

$$X_2 = \left(\frac{1}{E}\right) (\ell\sigma_2) \quad (7a.2)$$

$$(\sigma_1 - \sigma_2 + \sigma_3) = 0.0 \quad (7b)$$

where  $X_j(\bar{\chi})$ , the  $j$ th nodal displacement, and  $\sigma_i(\bar{\chi})$ , the  $i$ th element stress, are related to the behavior constraints and are functions of the three-component design variable  $\bar{\chi}$  (the areas of the elements). Here,  $\ell$  is the length of the second element (see fig. 1).

Note that these relationships hold for all values of the design variable (since  $\chi_i$  does not appear explicitly in eqs. (7)). Furthermore, linear functional dependence (or independence) of a set of behavior variables  $\{\sigma_i, X_j\}$  implies the linear dependence (or independence) of their associated constraint gradients (ref. 5).

Since we have three equations in five unknown functions ( $\sigma_1, \sigma_2, \sigma_3, X_1$ , and  $X_2$ ), given any two of the five functions (except for the  $\sigma_2, X_2$  pair), the other three functions can be determined. The observation that any set of more than two constraints is linearly functionally dependent corresponds to

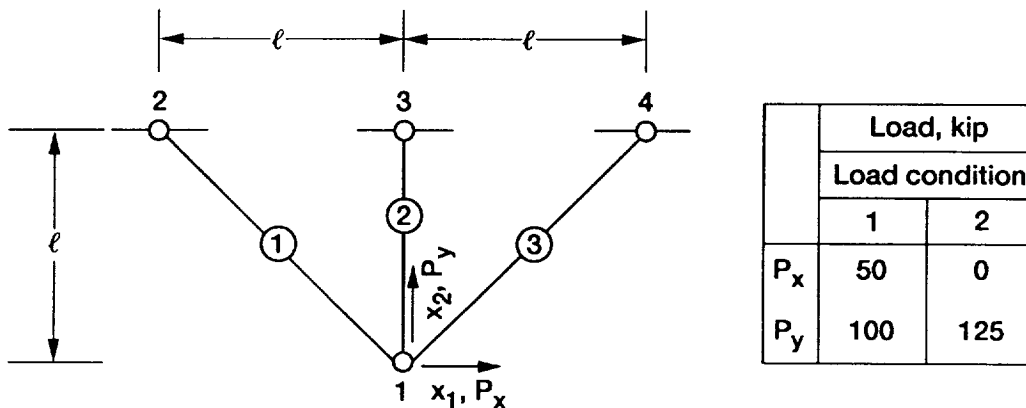


Figure 1.—Three-bar truss. (Elements are circled, nodes are not.)

TABLE I.—RANKS OF SEVERAL CONSTRAINT-GRADIENT MATRICES FOR THE THREE-BAR TRUSS  
[Element areas: 1.00, 9.30, and 3.67 in.<sup>2</sup>]

Case	Constraint set		Rank of constraint-gradient matrix	Nature of singularity
	Number	Constraints		
1	5	$\{\sigma_1, \sigma_2, \sigma_3, X_1, X_2\}$	2	Global
2	3	$\{\sigma_1, \sigma_2, \sigma_3\}$	2	Global and local
3	2	$\{\sigma_2, X_2\}$	1	Local

the global singularity condition identified earlier (refs. 1 to 3). The linear functional dependence among stresses, also noted earlier (refs. 2 and 3), is clearly indicated by equation (7b). Use of the knowledge of this global singularity to restrict the active constraint set to two constraints is, however, insufficient to guarantee linear functional independence. In particular, equation (7a.2) involves only one element stress ( $\sigma_2$ ) and one nodal displacement ( $X_2$ ) that would produce a singularity because of their linear functional dependence. We would expect, then, that the rank of the constraint-gradient matrix formed by (1) taking all five constraints would be two, (2) taking the three stress constraints would certainly be two, and (3) taking  $\sigma_2$  and  $X_2$  would be one. Table I shows the results of performing a singular value decomposition on the three constraint-gradient matrices indicated.

#### Use of the IFM Equations for Identification of Singularities

The integrated force method (IFM) is a structural analysis tool based on the method of forces through which global singularities in structural optimization were identified earlier (refs. 1 to 3). It will be used here to identify additional types of singularities.

Let us consider, more generally, an arbitrary truss under a single load condition that has  $n$  stress degrees of freedom and  $m$  displacement degrees of freedom. We will designate this structure as truss ( $n, m$ ), following the convention in the IFM (ref. 6). The following relations can be derived from the governing equations used in the IFM (see appendix B):

$$\bar{\sigma} = [\bar{B}] \bar{X} \quad (8a)$$

$$\bar{X} = [\bar{J}] \bar{\sigma} \quad (8b)$$

$$\bar{0} = [\bar{C}] \bar{\sigma} \quad (8c)$$

where the matrices  $[\bar{B}]$ ,  $[\bar{J}]$ , and  $[\bar{C}]$  are independent of the design variables; have full ranks of  $m$ ,  $m$ , and  $r$ , respectively; have dimensions of  $n \times m$ ,  $m \times n$ , and  $r \times n$ , respectively; and  $r = n - m$ . The choice of design variables depends on the structural elements chosen for the design, but typically these variables are taken as the element cross-sectional areas for truss elements, the moments of inertia for flexural elements, and

the shear area and polar moment of inertia for elements with torsion.

Equation (8a) is referred to as the set of stress-displacement relations and is derived from the force equilibrium equations. Equation (8b) describes the displacement-stress relations. Equation (8c) is the set of stress compatibility conditions. We note here that equations (8b) and (8c) can be used to derive equation (8a), and vice-versa. From the stress compatibility conditions (eq. (8c)), we can see that the set of all stress constraints is linearly functionally dependent. These equations are also consistent with the observation regarding global singularities made earlier (that the maximum number of stress and displacement constraints which can form a set of linearly independent functions is  $m$ ) (ref. 1). However, more subtle cases of singularities can arise by linear functional dependence among subsets of stress constraints (see eq. (8c)) or stress and displacement constraints (see eq. (8a) or (8b)). These singularities will be referred to as local singularities, since the relations are derived by consideration of local segments of the structure. This localization is reflected in the banded nature of the equilibrium and compatibility matrices,  $[\bar{B}]$  and  $[\bar{C}]$ , respectively.

#### Constraint Dependence for a 20-Bay Truss

For a more comprehensive example of how easily these more subtle forms of singularities can arise, consider the 20-bay truss shown in figure 2. The truss(101,80) consists of 20 bays, each defined by six adjunct elements. The truss has 101 elements and has 101 stress and 80 displacement degrees of freedom. It has 21 compatibility conditions ( $n - m = 21$ ). Using the evidence found earlier of possible global singularities, one should restrict the set of active constraints to be no more than the number of displacement degrees of freedom ( $m = 80$ ). The first two cases in table II show the rank of the resulting gradient matrix when more than 80 constraints are active. One might consider the restriction of limiting the number of active constraints to 80 (out of the maximum of 181 prescribed behavior constraints) to be rather mild since it might be expected that fewer than 80 constraints would be active, anyway. However, this restriction is insufficient to prevent all singularities that can arise.

Consider, first, the stress-displacement relations of the structure, which are defined through the modified equilibrium matrix  $[\bar{B}]$ . A few typical stress-displacement relations for the truss (101,80) are as follows:

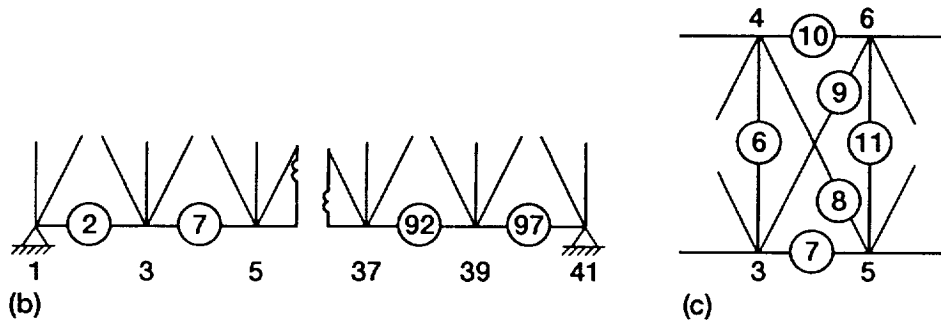
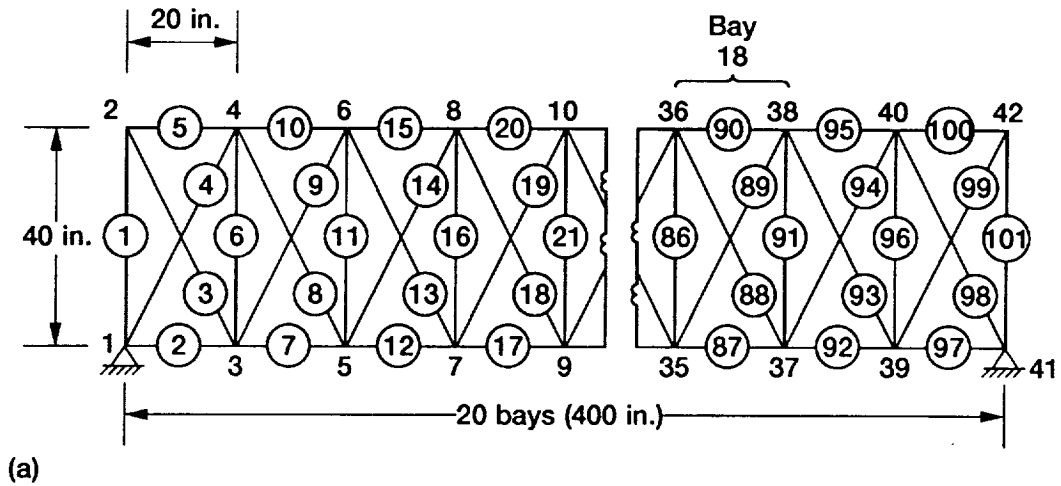
$$\sigma_1 = \bar{b}_{1,2} X_2 \quad (9a)$$

$$\sigma_4 = \bar{b}_{4,5} X_5 + \bar{b}_{4,6} X_6 \quad (9b)$$

$$\sigma_{88} = \bar{b}_{88,69} X_{69} + \bar{b}_{88,70} X_{70} + \bar{b}_{88,71} X_{71} + \bar{b}_{88,72} X_{72} \quad (9c)$$

$$\sigma_{90} = \bar{b}_{90,69} X_{69} + \bar{b}_{90,73} X_{73} \quad (9d)$$

From Figure 2, we can see that the stress in element 1,  $\sigma_1$ , and the vertical displacement at node 2,  $X_2$ , are directly



(a) Overall view.  
 (b) View showing the flexural load path under gravity load.  
 (c) View of bay 2.

Figure 2.—20-bay truss. Displacement constraint numbering for all nodes  $i$  such that  $2 \leq i \leq 40$  is as follows: (1) for horizontal displacements, the constraint index is  $2(i - 1) - 1$ ; (2) for vertical displacements, the constraint index is  $2(i - 1)$ . (Elements are circled, nodes are not.)

related as in equation (9a). Similarly, equation (9c) can be derived by examining the connectivity of element 88 in the 18th bay in figure 2. The stress in that element  $\sigma_{88}$  can be determined from the horizontal and vertical components of the displacements at node 36,  $X_{69}$  and  $X_{70}$ , and at node 37,  $X_{71}$  and  $X_{72}$ . The other relations can be derived in a similar way. Since each relation is derived by examining a small subset of the structure, the bandwidth of the  $[\bar{B}]$  matrix will be small, and the singularities produced can be considered to be local singularities.

The element areas, which are the design variables for this problem, do not appear explicitly in equations (9), since the coefficients are independent of those areas. Taking, as examples, the sets of constraints  $\{\sigma_1, X_2\}$ ,  $\{\sigma_4, X_5, X_6\}$ ,  $\{\sigma_{88}, X_{69}, X_{70}, X_{71}, X_{72}\}$ , and  $\{\sigma_{90}, X_{69}, X_{73}\}$  as active constraint sets, would produce rank-deficient gradient matrices  $[\nabla g]$  and singular  $[H]$  matrices (see cases 3 to 6 in table II for numerical verification). These clearly demonstrate that subsets containing many fewer active constraints than the global singularity restriction of at most 80 stress and displacement constraints can cause singularities. Next, consider the stress compatibility

conditions (CC) of the truss(101,80), which includes one external CC and 20 individual bay CC. The external CC, which has 20 terms, has the following form:

$$\bar{c}_{1,2}\sigma_2 + \bar{c}_{1,7}\sigma_7 + \bar{c}_{1,12}\sigma_{12} + \dots + \bar{c}_{1,97}\sigma_{97} = 0 \quad (10a)$$

The 20 individual bay compatibility conditions, each of which involves six stresses, have the following cyclic form:

$$\bar{c}_{2,1}\sigma_1 + \bar{c}_{2,2}\sigma_2 + \bar{c}_{2,3}\sigma_3 + \bar{c}_{2,4}\sigma_4 + \bar{c}_{2,5}\sigma_5 + \bar{c}_{2,6}\sigma_6 = 0 \quad (10b.1)$$

$$\bar{c}_{3,6}\sigma_6 + \bar{c}_{3,7}\sigma_7 + \bar{c}_{3,8}\sigma_8 + \bar{c}_{3,9}\sigma_9 + \bar{c}_{3,10}\sigma_{10} + \bar{c}_{3,11}\sigma_{11} = 0 \quad (10b.2)$$

$$\vdots$$

$$\bar{c}_{21,96}\sigma_{96} + \bar{c}_{21,97}\sigma_{97} + \bar{c}_{21,98}\sigma_{98} + \bar{c}_{21,99}\sigma_{99} + \bar{c}_{21,100}\sigma_{100} + \bar{c}_{21,101}\sigma_{101} = 0 \quad (10b.20)$$



TABLE II.—RANKS OF SEVERAL CONSTRAINT-GRADIENT MATRICES FOR THE 20-BAY TRUSS  
 [The element areas are pseudorandom numbers between 1.0 and 11.0 in.<sup>2</sup>]

Case	Constraint set		Rank of constraint-gradient matrix	Nature of singularity
	Number	Constraints		
1	181	{All stresses and displacements}	80	Global
2	101	{All stresses}	80	Global
3	2	{ $\sigma_1, X_2$ }	1	Local
4	3	{ $\sigma_4, X_5, X_6$ }	2	↓
5	5	{ $\sigma_{88}, X_{69}, X_{70}, X_{71}, X_{72}$ }	4	
6	3	{ $\sigma_{90}, X_{69}, \sigma_{73}$ }	2	
7	6	{ $\sigma_1, \sigma_2, \dots, \sigma_6$ }	5	
8	8	{ $\sigma_1, \sigma_2, \dots, \sigma_6, \sigma_{20}, X_{60}$ }	7	
9	6	{ $\sigma_{31}, \sigma_{32}, \dots, \sigma_{36}$ }	5	
10	20	{ $\sigma_2, \sigma_7, \sigma_{12}, \dots, \sigma_{97}$ }	19	

Again, these relations (eq. (10)) are independent of the design variables. The sparsity, and (in the case of the 20 bay compatibility conditions) the bandedness, of the  $[\bar{C}]$  matrix is produced from the localized character of the relations. The external CC (eq. (10a)) ensures that the total deformation between the two boundaries (nodes 1 and 41) is zero (see fig. 2(b)). The 20 bay CC's ensure that the bars which form the bay deform in a consistent manner, such that all bars fit together before and after deformations, without inducing any residual strains (see, for example, fig. 2(c)).

Taking the first six stress constraints  $\{\sigma_1, \sigma_2, \dots, \sigma_6\}$  will produce a constraint-gradient matrix with a rank less than six (see case 7, table II). In fact, taking any set of constraints that include these six will produce a rank-deficient constraint-gradient matrix (e.g., see case 8, table II). Other examples of singularities can be produced with sets of constraints that include  $\{\sigma_{31}, \sigma_{32}, \dots, \sigma_{36}\}$  or  $\{\sigma_2, \sigma_7, \sigma_{12}, \dots, \sigma_{97}\}$ . These have also been verified numerically (see cases 9 and 10, table II). Note, here, that the 20 stresses  $\{\sigma_2, \sigma_7, \sigma_{12}, \dots, \sigma_{97}\}$  correspond to the flexural load path for the structure under gravity loads and therefore are very likely to all become active, creating singularities during structural optimization procedures.

## Discussion

We have seen how singularities can (sometimes quite easily) arise in structural optimization because of rank deficiencies in constraint-gradient matrices that are used in mathematical programming techniques to determine new search directions. In some variants of these algorithms, starting from an identity matrix, the matrix  $[H]$  or related matrices are constructed by using constraint gradients following an update procedure (ref. 4). Often these matrices are initially well behaved, but become poorly conditioned (or singular) as the solution approaches the optimal point, thus requiring re-initialization. Noting that, typically, few constraints are active initially and

that many may be active near the optimal solution, it is reasonable to hypothesize that the singularities observed are due to linear dependence among the active constraints. Once again, it seems very important to ensure that the active constraints chosen constitute a linearly independent set of functions.

Although generating conditions in which singularities can arise is very easy using equations (8), producing an algorithm to ensure linear functional independence among stress and displacement constraints is not so straightforward. One naive approach, which would be applicable to any structural analysis formulation, might be to find the rank of the matrix formed by the gradients of the active constraint set. If this matrix were rank deficient, the offending constraint(s) could be deleted, or replaced with some "less active," but (what one would hope are) independent, constraint(s).

A far less costly, and more elegant, approach would be to examine the stress-displacement relations, the displacement-stress relations, and the compatibility conditions of the IFM (eqs. (8)). Although the stress-displacement relations alone would be sufficient, it would often be advantageous to use one, or both, of the other two relationships. For example, when only stress constraints occur in the active constraint set, examination of the CC alone would be sufficient to determine whether or not the set was linearly functionally independent. Details on a procedure to ensure linear functional independence among active constraints will not be given here, but will be provided in a subsequent paper (Guptill, J.D.; Patnaik, S.N.; and Berke, L.: Identification and Preclusion of Singularities during Structural Optimization; to be published).

## Multiple Load Conditions

With multiple load conditions that are mutually independent, it can be shown that the stress gradients for any single element are mutually independent. To illustrate this result with a simple numerical example, we took two load conditions for the three-

TABLE III.—RANKS OF SEVERAL CONSTRAINT-GRADIENT MATRICES FOR MULTIPLE LOAD CONDITIONS  
[Element areas: 1.00, 9.30, and 3.67 in.<sup>2</sup>]

Case	Constraint set		Rank of constraint-gradient matrix	
	Number	Load conditions <sup>a</sup>		
		1		2
1	2	$\{\sigma_1\}$	$\{\sigma_1\}$	2
2	2	$\{\sigma_2\}$	$\{X_2\}$	2
3	3	$\{\sigma_1, \sigma_2\}$	$\{\sigma_3\}$	3

<sup>a</sup>Load conditions are defined in figure 1

bar truss shown in figure 1. The linear independence of the stress gradients associated with the first element under the two load conditions is demonstrated in table III. Furthermore, although  $\sigma_2$  and  $X_2$  were found to be linearly functionally dependent under one load condition, taking  $\sigma_2$  from load condition 1 and  $X_2$  from load condition 2 produces a gradient matrix of full rank (see table III). Moreover, taking two linearly functionally independent constraints from one load condition and one from another produces a gradient matrix of rank three. An example of this is also shown in table III.

### Frequency Constraints

Frequency constraints appear to be linearly functionally independent of stress and displacement constraints. The frequency constraint  $f$  is inversely proportional to the frequency  $\omega$  where

$$\omega^2 = \frac{\bar{X}_\omega^T [K] \bar{X}_\omega}{\bar{X}_\omega^T [M] \bar{X}_\omega} = \frac{\bar{F}_\omega^T [S] \bar{F}_\omega}{\bar{F}_\omega^T [M^{-1}] \bar{F}_\omega} \quad (11)$$

and  $\bar{X}_\omega$ ,  $[K]$ , and  $[M]$  are the displacement mode shape, the stiffness matrix, and the mass matrix, respectively, associated with the displacement method (ref. 8); and  $\bar{F}_\omega$ ,  $[S]$ , and  $[M^{-1}]$  are the force mode shape, the IFM governing matrix, and the IFM mass matrix, respectively (ref. 9). It seems unlikely that the frequency constraint could ever be written as a linear combination of the stress and displacement constraints. Numerical examples indicating the linear independence of frequency constraint gradients are shown in Table IV.

### Structures Other Than Trusses

For nontruss structures, the complexity is increased for several reasons, including (1) the presence of more than one design variable per element, (2) the presence of multi-axial

TABLE IV.—RANKS OF SEVERAL CONSTRAINT-GRADIENT MATRICES IN THE PRESENCE OF FREQUENCY CONSTRAINTS  
[Element areas: 1.00, 9.30, and 3.67 in.<sup>2</sup>]

Case	Constraint set		Rank of constraint-gradient matrix	
	Number	Constraints	With frequency constraints	Without frequency constraints
1	6	$\{\sigma_1, \sigma_2, \sigma_3, X_1, X_2, f\}$	3	2
2	4	$\{\sigma_1, \sigma_2, \sigma_3, f\}$	3	2
3	3	$\{\sigma_2, X_2, f\}$	2	1

stress states, and (3) more complicated IFM equations. An initial introduction to the complexity of singularity issues for nontruss structures has been reported (ref. 9).

## Conclusions

Singularity conditions can arise in structural optimization because of linear functional dependence among active stress and displacement constraints. These conditions can be global or local in nature. Local singularities can occur more frequently than global singularities. Linear functional dependence can be seen among sets of constraints containing very small percentages of the prescribed behavior constraints.

The presence of linear functional dependence can best be determined by examination of the equations derived in the integrated force method. If the active constraint set is composed of stress constraints only, examination of the IFM compatibility conditions is sufficient. When the active constraint set includes both stress and displacement constraints, either the stress-displacement relations or a combination of displacement-stress relations and the compatibility conditions need to be examined. Frequency constraints appear to be linearly functionally independent of the stress and displacement constraints. Stress and displacement constraints that cross multiple (mutually independent) load conditions are linearly functionally independent. Although more complicated, it would be of benefit to extend this analysis of singularities to nontruss structures.

Lewis Research Center  
National Aeronautics and Space Administration  
Cleveland, Ohio, November 12, 1991

## Appendix A Symbols

$A_i$	cross-sectional area of the $i$ th element	$\bar{P}^*$	modified load vector
$[B]$	equilibrium matrix	$r$	number of strain compatibility conditions
$[\tilde{B}]$	modified equilibrium matrix	$[S]$	IFM governing matrix
$\tilde{b}_{i,j}$	$(i,j)$ th element of the modified equilibrium matrix	$\bar{X}$	displacement vector
$[C]$	compatibility matrix	$X_j$	$j$ th nodal displacement
$[\tilde{C}]$	modified compatibility matrix	$X_\omega$	displacement mode shape associated with the displacement method
$\tilde{c}_{i,j}$	$(i,j)$ th element of the modified compatibility matrix	$\{\alpha_j\}$	set of constants
$E$	Young's modulus	$\bar{\beta}$	deformation vector
$E_i$	Young's modulus of the $i$ th element	$\bar{\beta}_0$	initial deformation vector
$[E_i]$	diagonal matrix of Young's moduli scaled with lengths	$\delta\bar{R}$	effective initial deformation vector
$\bar{F}$	internal forces	$i$	node number
$\bar{F}_\omega$	force mode shape associated with IFM frequency analysis	$\kappa$	number of active constraints used in the calculation of the direction vector
$f$	frequency constraint	$\lambda_0$	scaling factor
$[G]$	concatenated flexibility matrix	$\bar{\sigma}$	stress vector
$g_j$	$j$ th constraint value	$\sigma_0$	strength
$[H]$	coefficient matrix in a method of feasible directions	$\sigma_i$	stress of the $i$ th element
$[I]$	identity matrix	$\bar{\chi}$	design variable vector
$[J]$	deformation coefficient matrix	$\chi_i$	$i$ th design variable
$[\tilde{J}]$	modified deformation coefficient matrix	$\bar{\varphi}$	direction vector
$[K]$	stiffness matrix associated with the displacement method	$\omega$	frequency
$\ell$	characteristic dimension of the three-bar truss	$\bar{0}$	null vector
$\ell_i$	length of the $i$ th element	$\bar{\nabla}f$	gradient of the merit function
$[M]$	mass matrix associated with the displacement method	$[\nabla g]$	constraint-gradient matrix
$[M^T]$	IFM mass matrix	$\nabla g_j$	gradient of the $j$ th constraint
$m$	number of displacement degrees of freedom	$\partial g_j / \partial \chi_i$	partial derivative of the $j$ th constraint with respect to the $i$ th design variable
$n$	number of design variables; number of stress degrees of freedom	$[\cdot]^T$	transpose of a matrix
$\bar{P}$	load vector	$[\cdot]^{-1}$	inverse of a matrix
		$[\cdot]^{-T}$	inverse transpose of a matrix

## Appendix B

### Key Integrated Force Method Equations

The key equations of the integrated force method (IFM) as related to the singularity issue are presented in this appendix. The IFM considers all the internal  $n$  forces,  $\vec{F}$ , as the simultaneous unknowns. The  $m$  force equilibrium equations,  $[B]\vec{F} = \vec{P}$ , and the  $r$  strain compatibility conditions,  $[C][G]\vec{F} = \vec{0}$ , are concatenated to obtain the governing equations of the method (refs. 10 and 11) as

$$\begin{bmatrix} [B] \\ [C][G] \end{bmatrix} \vec{F} = \begin{bmatrix} \vec{P} \\ \delta\vec{R} \end{bmatrix} \text{ or } [S]\vec{F} = \vec{P}^* \quad (B1)$$

where  $[B]$  is the  $m \times n$  equilibrium matrix,  $[C]$  is the  $r \times n$  compatibility matrix,  $[G]$  is the  $n \times n$  concatenated flexibility matrix that links deformations  $\vec{\beta}$  to forces  $\vec{F}$  as ( $\vec{\beta} = [G]\vec{F}$ ),  $\vec{P}$  is the  $m$ -component load vector,  $\delta\vec{R}$  is the  $r$ -component effective initial deformation vector defined as  $\delta\vec{R} = -[C]\vec{\beta}_0$ ,  $\vec{\beta}_0$  is the  $n$ -component initial deformation vector,  $[S]$  is the  $n \times n$  governing matrix, and  $m + r = n$ . The matrices  $[B]$ ,  $[C]$ ,  $[G]$ , and  $[S]$  are banded and have full row ranks of  $m$ ,  $r$ ,  $n$ , and  $n$ , respectively. For simplicity, initial deformations are neglected here ( $\vec{\beta}_0 = \vec{0}$ ).

The solution of equation (B1) yields the  $n$  forces,  $\vec{F}$ . The  $m$  displacements,  $\vec{X}$ , are obtained from the forces by

$$\vec{X} = [J][G]\vec{F} \quad (B2)$$

where  $[J]$  is the  $m \times n$  deformation coefficient matrix defined as ( $[J] = m$  rows of  $[S]^{-T}$ ). For static analysis, the matrix  $[J]$  is independent of element areas. For trusses, the flexibility matrix  $[G]$  is a diagonal matrix, and its elements are

$$g(i,i) = \frac{\ell_i}{A_i E_i} \quad \text{for } i = 1, 2, \dots, n \quad (B3)$$

where  $\ell_i$  is the length of the  $i$ th element,  $A_i$  is the area of the  $i$ th element, and  $E_i$  is the Young's modulus of the  $i$ th element.

#### Stress-Displacement Relations

The stress-displacement relations can be obtained from the general relations ( $\vec{\beta} = [G]\vec{F} = [B]^T\vec{X}$ ) with appropriate specialization for trusses as

$$\vec{\sigma} = [\tilde{B}]\vec{X} \quad (B4)$$

where  $[\tilde{B}]$  is a sparse, banded matrix with  $[\tilde{B}] = [E_i][B]^T$ , and  $E_i/\ell_i$  are the nonzero elements of the diagonal matrix  $[E_i]$ .

#### Displacement Stress Relations

The displacements  $\vec{X}$  can be written in terms of the stresses as

$$\vec{X} = [\tilde{J}]\vec{\sigma} \quad (B5)$$

where  $[\tilde{J}] = [J][E_i]^{-1}$ .

#### Compatibility Conditions in Terms of Stresses

The strain compatibility conditions ( $[C][G]\vec{F} = \vec{0}$ ) can be written as stress compatibility conditions:

$$[\tilde{C}]\vec{\sigma} = \vec{0} \quad (B6)$$

where  $[\tilde{C}]$  is a sparse matrix with  $[\tilde{C}] = [C][E_i]^{-1}$ . The  $[\tilde{B}]$ ,  $[\tilde{J}]$ , and  $[\tilde{C}]$  matrices can all be considered independent of element areas for static analysis.

## References

1. Patnaik, S.N.: Behavior of Trusses with Stress and Displacement Constraints. *Comput. Struct.*, vol. 22, no. 4, 1986, pp. 619-623.
2. Patnaik, S.N.; and Dayaratnam, P.: Behavior and Design of Pin-Connected Structures. *Int. J. Numer. Methods Eng.*, vol. 2, no. 4, 1970, pp. 579-595.
3. Dayaratnam, P.; and Patnaik, S.N.: Feasibility of Full Stress Design. *AIAA J.*, vol. 7, no. 4, 1969, pp. 773-774.
4. Gallagher, R.H.; and Zienkiewicz, O.C., eds.: *Optimum Structural Design*. John Wiley & Sons, 1973.
5. Patnaik, S.N.; and Gallagher, R.H.: Gradients of Behavior Constraints and Reanalysis Via the Integrated Force Method. *Int. J. Numer. Methods Eng.*, vol. 23, no. 12, 1986, pp. 2205-2212.
6. Patnaik, S.N.; Berke, L.; and Gallagher, R.H.: Integrated Force Method Versus Displacement Method for Finite Element Analysis. *Comput. Struct.*, vol. 38, no. 4, 1991, pp. 377-407.
7. Reklaitis, G.V.; Ravindran, A.; and Ragsdell, K.M.: *Engineering Optimization: Methods and Applications*. John Wiley & Sons, 1983.
8. Zienkiewicz, O.C.: *The Finite Element Method in Engineering Science*. McGraw-Hill, New York, 1977.
9. Patnaik, S.N.; and Yadagiri, S.Y.: Design for Frequency by the Integrated Force Method. *Comput. Methods Appl. Mech. Eng.*, vol. 16, no. 2, 1978, pp. 213-230.
10. Patnaik, S.N.; Berke, L.; and Gallagher, R.H.: Compatibility Conditions of Structural Mechanics for Finite Element Analysis. *AIAA J.* vol. 29, no. 5, 1991, pp. 820-829.
11. Patnaik, S.N.: Variational Energy Formulation for the Integrated Force Method. *AIAA J.*, vol. 24, no. 1, 1986, pp. 129-137.

REPORT DOCUMENTATION PAGE			Form Approved OMB No. 0704-0188	
Public reporting burden for this collection of information is estimated to average 1 hour per response, including the time for reviewing instructions, searching existing data sources, gathering and maintaining the data needed, and completing and reviewing the collection of information. Send comments regarding this burden estimate or any other aspect of this collection of information, including suggestions for reducing this burden, to Washington Headquarters Services, Directorate for Information Operations and Reports, 1215 Jefferson Davis Highway, Suite 1204, Arlington, VA 22202-4302, and to the Office of Management and Budget, Paperwork Reduction Project (0704-0188), Washington, DC 20503.				
1. AGENCY USE ONLY (Leave blank)	2. REPORT DATE March 1992	3. REPORT TYPE AND DATES COVERED Technical Memorandum		
4. TITLE AND SUBTITLE Singularities in Optimal Structural Design			5. FUNDING NUMBERS WU-307-50-00	
6. AUTHOR(S) S.N. Patnaik, J.D. Guptill, and L. Berke				
7. PERFORMING ORGANIZATION NAME(S) AND ADDRESS(ES) National Aeronautics and Space Administration Lewis Research Center Cleveland, Ohio 44135-3191			8. PERFORMING ORGANIZATION REPORT NUMBER E-6686	
9. SPONSORING/MONITORING AGENCY NAME(S) AND ADDRESS(ES) National Aeronautics and Space Administration Washington, D.C. 20546-0001			10. SPONSORING/MONITORING AGENCY REPORT NUMBER NASA TM-4365	
11. SUPPLEMENTARY NOTES S.N. Patnaik, Ohio Aerospace Institute, 2001 Aerospace Parkway, Brook Park, Ohio 44142; J.D. Guptill and L. Berke, NASA Lewis Research Center. Responsible person, S.N. Patnaik, (216) 433-8368.				
12a. DISTRIBUTION/AVAILABILITY STATEMENT Unclassified - Unlimited Subject Category 39			12b. DISTRIBUTION CODE	
13. ABSTRACT (Maximum 200 words)  Singularity conditions that arise during structural optimization can seriously degrade the performance of the optimizer. The singularities are intrinsic to the formulation of the structural optimization problem and are not associated with the method of analysis. Certain conditions that give rise to singularities have been identified in earlier papers, along with a proposition to alleviate the consequences of their presence. <sup>1-3</sup> These singularities were global in nature, encompassing the entire structure. Further examination revealed more complex sets of conditions in which singularities occur. Some of these singularities are local in nature, being associated with only a segment of the structure. Moreover, the likelihood that one of these local singularities may arise during an optimization procedure can be much greater than that of the global singularity identified earlier. This paper provides examples of these additional forms of singularities. It also gives a framework in which these singularities can be recognized. In particular, the singularities can be identified by examination of the stress-displacement relations along with the compatibility conditions and/or the displacement-stress relations derived in the integrated force method of structural analysis.				
14. SUBJECT TERMS Structures; Optimization; Singularity (mathematics); Stresses; Displacement; Frequencies; Compatibility; Equilibrium; Sensitivity; Constraints; Structural design			15. NUMBER OF PAGES 12	
			16. PRICE CODE A03	
17. SECURITY CLASSIFICATION OF REPORT Unclassified	18. SECURITY CLASSIFICATION OF THIS PAGE Unclassified	19. SECURITY CLASSIFICATION OF ABSTRACT Unclassified	20. LIMITATION OF ABSTRACT	